Fuster et al, http://www.jgp.org/cgi/doi/10.1085/jgp.200810016

SUPPLEMENTAL MATERIAL

Here, we describe efforts to monitor and quantify proton fluxes in giant excised patches and to define NHE activities in excised patches. From this work we conclude that significant complexities of the excised patch configuration hinder accurate determination of proton fluxes and that NHE activity is in some way disrupted by formation of gigaseals, probably as a result of membrane stretch as the membrane is pulled into the pipette tip. Methods used were as described in the article. Solutions used are described below.

SOLUTIONS

Figure S1

Bath solution: 140 NaCl, 2 $MgCl_2$, 10 Tris, pH 6.0 or 8.0; pipette solution: 140 NaCl, 2 $MgCl_2$, 0.1 Tris, pH 7.0; pipette solution: 60 KOH, 30 l-aspartate acid, 10 KCl, 1 EGTA, 0.5 $MgCl_2$, 10 MgATP, 50 Mes, pH 6.0, 50 Pipes, pH 6.8, 50 Mops, pH 7.2, and 50 HEPES, pH 7.6. Bath and pipette solutions contained 10 µM 3,3′,4',5-tetrachlorosalicylanilide (TCS), which was obtained from Acros Organics through Fisher Scientific.

Figure S2

Bath solution: 140 CsCl, 1 EGTA, 1 $MgCl_2$, 20 Mes, pH 6.5; pipette solution: 140 CsCl, 2 $CaCl_2$, 1 $MgCl_2$, 0.1 HEPES, pH 7.5.

Figure S3.

Bath and on-cell pipette solution: 140 NaCl, 2 $CaCl_2$, 2 $MgCl_2$, 0.1 Tris, pH 8.0; whole cell pipette solution: 120 KOH, 120 l-aspartate acid, 1 EGTA, 0.5 $MgCl_2$, 10 MgATP, 20 Mes, pH 6.5.

Proton Flux Calculations

The calculation of ion fluxes from ion gradients was performed as described previously (Kang et al., 2003; Fuster et al., 2004).

Proton Gradients Are Attenuated in the Excised Patch Model

The giant membrane patch is an advantageous experimental model for mechanism-oriented transport studies because it allows rigorous control of solutions on both membrane sides and free access to the cytoplasmic side (Hilgemann and Lu, 1998). In whole cell recording with CHO cells, NHE1-mediated proton fluxes can exceed 20-pA equivalents(Fuster et al., 2004), allowing us to predict that proton fluxes would be easily recorded in excised patches via intra-patch pipette pH electrodes. As described in Figs. S1–S3, however, we detect no NHE activities in excised patches, and we made substantial efforts to address the underlying reasons.

To evaluate whether proton fluxes can be accurately determined using the excised patch model (see upper cartoon in both panels), we first used multiple protonophores to attempt to establish electrogenic proton fluxes in excised patches, the magnitudes of which could be used to predict proton gradients via diffusion simulations. From bilayer
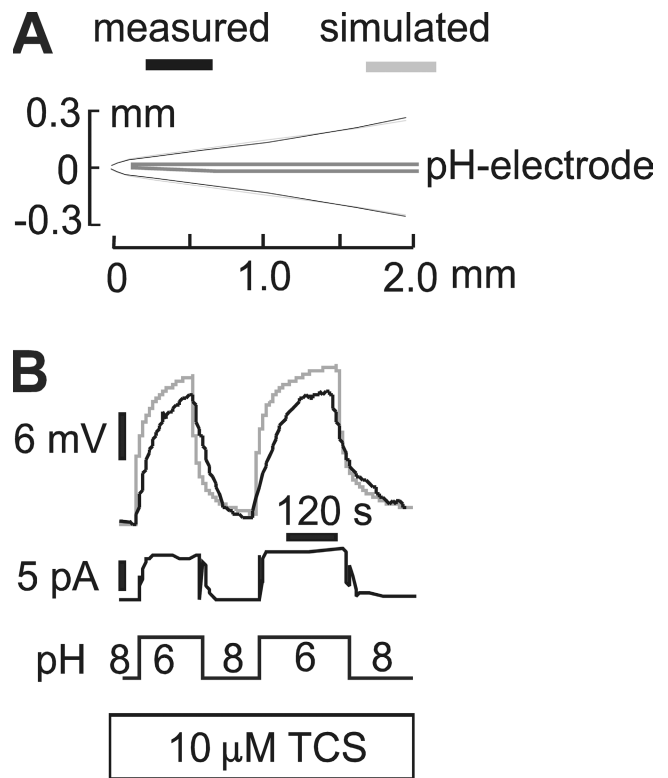

Figure S1. Measurement and simulation of intra-pipette, protonophore-induced proton fluxes by pH microelectrode. (A) The patch pipette contained a pH microelectrode that was moved manually to a distance of 35 µm from the tip the pipette orifice. Bath and pipette solutions (see Materials and methods) both contained 10 µM of the protonophore, TCS. (B) Bath pH was changed between 8.0 and 6.0, and TCS-mediated proton fluxes (mV, black color) and currents (pA) were recorded simultaneously. Gray lines give simulated proton fluxes that assumed step-like changes of a proton current with an amplitude of 7 pA into a pipette with the dimensions given by the gray lines in A. See Materials and methods for details. Membrane potential was held at 0 mV throughout the experiment. This experiment is representative of four individual experiments.
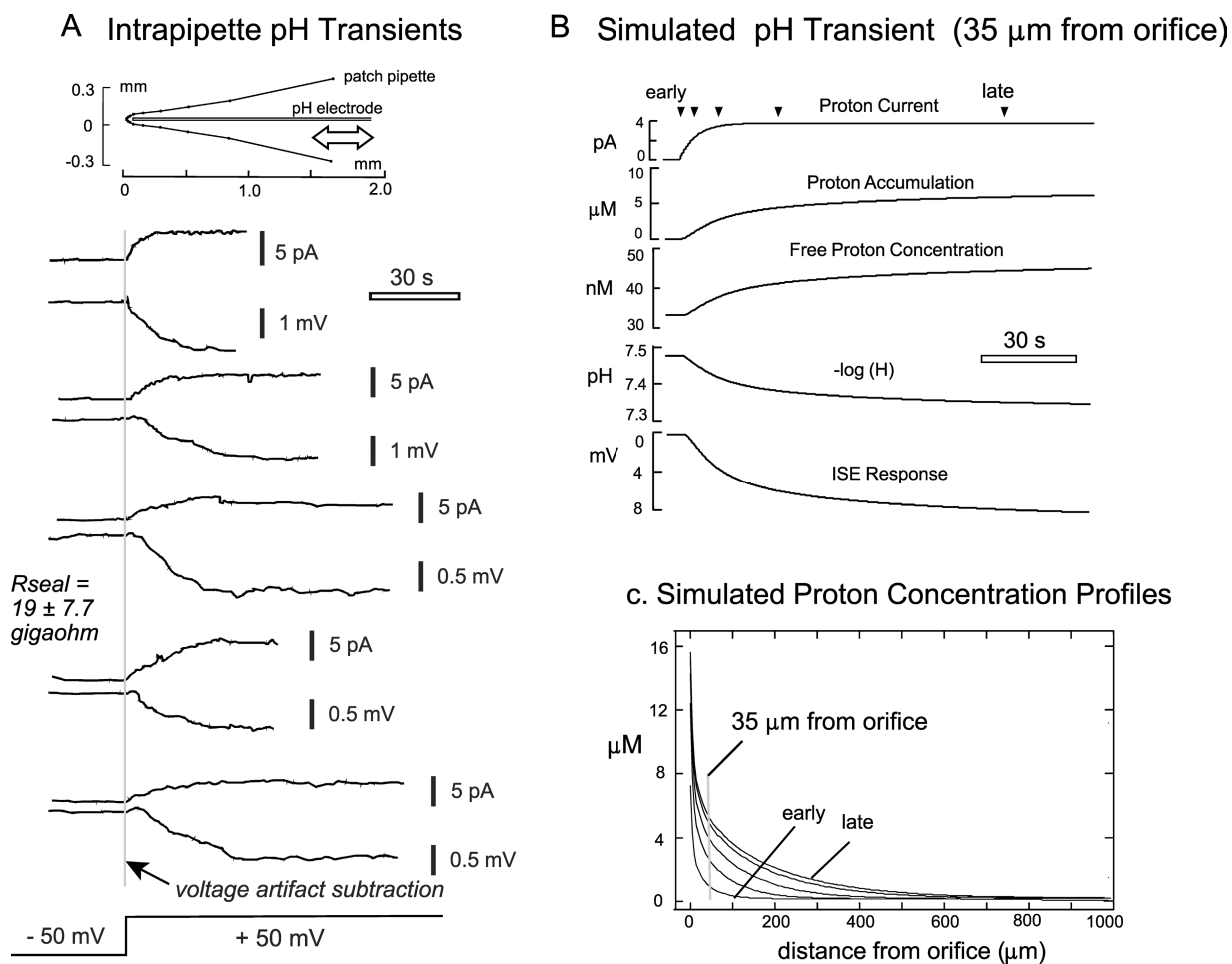
A Intrapipette pH Transients

B Simulated pH Transient (35 μm from orifice)

c. Simulated Proton Concentration Profiles

Figure S2. Measurement and simulation of intra-pipette, channel-induced proton fluxes by pH microelectrode. CHO-derived, plasmalemmal NHE-deficient AP-1 cells were transfected with C terminally GFP-tagged human voltaged-gated proton channel (HVCN1-GFP). 24 h after transfection, inside-out patches from HVCN1-GFP–expressing AP-1 cells were obtained and held at −50 mV. After pH microelectrodes were moved manually to a position 35 μm from the pipette orifice, the voltaged gated proton channels were activated by changing the voltage to +50 mV, and proton currents and intra-pipette proton fluxes were recorded simultaneously. (A) Individual records are from repetitive depolarization from the same inside-out patch. (B) Simulated pH transients with assumption of pipette geometry as determined in the experiment depicted in A. (C) Simulated proton concentration profile in dependence of distance from the pipette orifice for early and late (steady-state) time points (pipette geometry same as used for B).

studies (Benz and McLaughlin, 1983; Kasianowicz et al., 1984), the classical proton ionophores such as dinitrophenol (see upper cartoon in both panels), FCCP, and CCCP, would be expected to generate several pA of proton currents with favorable proton gradients in excised membrane patches with capacitances of 2–4 pF. However, protonophore activity of these probes appears to be inhibited by the presence of cholesterol in membranes (Starkov et al., 1994; Vianello et al., 1995), and accordingly, the activities of most protonophores are rather low in the surface membranes of most cells. Consistent with this notion, we were unable to generate significant proton conductances or gradients in giant excised patches from multiple cell types using the protonophores mentioned above (not depicted).

As illustrated in Fig. S1, we found that the protonophore, TCS (Bennekou, 1988), can indeed induce large proton currents and proton gradients in giant excised patches from multiple cell types. The results presented are from an excised CHO patch with a pipette tip diameter of 8 μm (see Fig. S1 A). Black lines give the pipette dimensions, and gray lines give the "fitted" dimensions used in the simulation. The pipette solution was buffered with 0.1 mM Tris, adjusted to pH 8.2. The intra-patch pH electrode tip was positioned at 35 μm from the pipette orifice. TCS was applied at a concentration of 10 μM for 2 min in a cytoplasmic solution buffered to pH 8.0 with 10 mM Tris. As shown in Fig. S1 B, outward membrane currents of 7–9 pA are rapidly activated and deactivated by applying and removing cytoplasmic solution buffered to a pH of 6.0 versus 8.0. The intra-pipette pH electrode (black record above the current record) detects an acidifying signal of ∼15 mV, which develops with an approximate time constant of 100 s, during activation
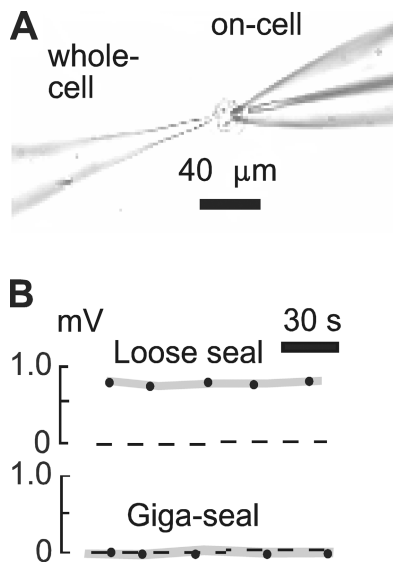
A

whole-cell

on-cell

40 μm

B

mV

30 s

Loose seal

1.0

0

1.0

Giga-seal

0

Figure S3. NHE1 activity is lost after gigaseal formation. (A) Double patch clamp experiment. A CHO cell is held in whole cell configuration (left), and a second patch pipette with an oscillating intra-pipette pH microelectrode (right) is used to obtain a loose or tight on-cell (giga Ohm seal) configuration. (B) Voltage difference detected by oscillating intra-pipette pH electrode (for details see Materials and methods). NHE1-induced proton flux is present during loose seal condition (upper panel) and detected as an ~0.8-mV signal by pH microelectrode. NHE1 transport activity is lost after gigaseal formation (lower panel).

of outward current, and the acidification dissipates with a similar time course. To test our ability to quantify proton fluxes, the pipette dimensions were determined carefully (see Fig. S1 A), and the results were simulated as described in Materials and methods (see gray record in Fig. S1 B). The simulation, performed with diffusion coefficients of 10^{-5} and 10^{-4} cm^2/s for Tris and protons, respectively, predicted a 15% larger proton gradient than determined experimentally.

Similar results, obtained with three other excised patches, appeared to validate reasonably the excised patch model for studies of proton fluxes. However, it appeared troublesome in these experiments that the activity of TCS dissipated quite rapidly after its washout, raising the possibility that an "electroneutral" proton flux might occur by rapid dissociation of ionophore–proton complexes from the extracellular membrane side. In addition, it was troublesome that the ionophore often disrupted patches and thereby might be expected to generate nonselective conductances as might be expected from studies of TCS in phospholipid bilayers (Barratt and Weaver, 1979).

For these reasons, it seemed essential to pursue another approach. As described in Fig. S2, we chose to express the recently cloned voltage-activated proton channel (Ramsey et al., 2006) in CHO cells. This channel activates over the course of several seconds upon depolarization from negative to positive potentials, and the reversal potentials of currents indicate that the ion translocation mechanism is highly proton selective. Fig. S2 A shows multiple records from a typical experiment in which the pipette solution was buffered with 0.1 mM HEPES to pH 7.5, while the cytoplasmic solution was buffered to pH 6.5 with 20 mM MES. The diagram in Fig. S2 A shows the patch pipette dimensions (inner tip diameter, 8.2 μm). Several current records from the same patch are presented with the simultaneous pH electrode recordings from a position 35 μm from the pipette orifice. The membrane capacitance was estimated to be 3 pF, and the average seal resistance was 19 ± 7.7 gigaohm. Immediate shifts of background current and electrode potential upon changing membrane potential were subtracted, as indicated by a gray line in the figure. Proton currents activate, as expected, with approximate time constants of 3–4 s at +50 mV with peak current magnitudes of 3–4 pA, and proton gradients develop within the patch pipette over the course of 20–50 s.

Fig. S2 B shows our simulations of proton fluxes occurring in this experiment, whereby a 4 pA proton current was simulated to activate with a time constant of 4 s. Diffusion coefficients for buffer and protons were assumed to be 10^{-5} and 10^{-4} cm^2/s, respectively. Simulations of total proton accumulation, the free proton concentration, the pH, and the ISE response are given for a point 35 μm from the pipette tip. Simulated proton concentration profiles occurring in the pipette tip are given in Fig. S2 C for the time points indicated above the simulated proton current in Fig. S2 B. An ISE response of >6 mV is predicted, corresponding to an acidification of somewhat more than 0.2 pH units. Here, as in all experiments with proton channels, the measured ISE response was at least three times smaller than the predicted response. As this discrepancy is much larger than discrepancies determined for measurements of Ca, Na, and K fluxes with these same methods (Kang and Hilgemann, 2004), we conclude that complexities of proton buffering (e.g., carbonate leeching) and/or diffusion (e.g., proton chaining along the glass) significantly dissipate proton gradients in the pipette. Up to now, we have not been able to determine clearly which factor is most important.

NHE1 Activity Is Disrupted by Membrane Stretch

Even if proton gradients in patch pipettes are attenuated by a factor of five from simple predictions, we can project that NHE-mediated proton fluxes would be clearly detectable in the patch pipette if flux densities are comparable to those in whole cell recording. Therefore, we performed experiments as described in Fig. S3 to test whether exchange activity might be disrupted in some way by seal formation. To do so, we initiated whole cell voltage clamp of CHO cells under conditions that generate nearly maximal proton fluxes in whole cell recording (cytoplasmic pH of

6.5 with 20 mM Mes; extracellular pH of 8.0 with 0.1 mM Tris). Then, we approached the cell with a patch pipette containing the same extracellular solution and an intra-pipette pH electrode positioned close to the tip. After approaching the cell and touching it with the patch pipette, a robust ~1-mV ISE signal could be defined by moving the pH electrode tip close to the patch pipette tip versus a position 50 μm higher in the patch pipette (see data for "loose seal" in Fig. S3 B). After ascertaining that the pH gradient was stable, a true gigaseal was formed by applying further suction to the patch pipette. Thereafter, oscillation of the pH electrode from a position very close to the cell membrane to a position 50 μm further away generated no detectable ISE signal (Fig. S3 B, bottom). From these results, we concluded that membrane perturbation by suction and gigaseal formation causes a complete loss of Na/H exchange activity in the membrane patches. The mechanism for this disruption remains elusive, and we were obligated to proceed to analyze Na/H exchange function in whole cell recording mode.

REFERENCES

Barratt, M.D., and A.C. Weaver. 1979. The interaction of 3,3′,4',5-tetrachlorosalicylanilide with phosphatidylcholine bilayers. *Biochim. Biophys. Acta.* 555:337–348. PubMed doi:10.1016/0005-2736(79)90172-X

Bennekou, P. 1988. Steady-state and transient membrane potentials in human red cells determined by protonophore-mediated pH changes. *J. Membr. Biol.* 106:41–46. PubMed doi:10.1007/BF01871765

Benz, R., and S. McLaughlin. 1983. The molecular mechanism of action of the proton ionophore FCCP (carbonylcyanide p-trifluoromethoxyphenylhydrazone). *Biophys. J.* 41:381–398. PubMed

Fuster, D., O.W. Moe, and D.W. Hilgemann. 2004. Lipid- and mechanosensitivities of sodium/hydrogen exchangers analyzed by electrical methods. *Proc. Natl. Acad. Sci. USA.* 101:10482–10487. PubMed doi:10.1073/pnas.0403930101

Hilgemann, D.W., and C.C. Lu. 1998. Giant membrane patches: improvements and applications. *Methods Enzymol.* 293:267–280. PubMed doi:10.1038/nature02271

Kang, T.M., and D.W. Hilgemann. 2004. Multiple transport modes of the cardiac Na+/Ca2+ exchanger. *Nature.* 427:544–548. PubMed doi:10.1038/nature02271

Kang, T.M., V.S. Markin, and D.W. Hilgemann. 2003. Ion fluxes in giant excised cardiac membrane patches detected and quantified with ion-selective microelectrodes. *J. Gen. Physiol.* 121:325–347. PubMed doi:10.1085/jgp.200208777

Kasianowicz, J., R. Benz, and S. McLaughlin. 1984. The kinetic mechanism by which CCCP (carbonyl cyanide m-chlorophenylhydrazone) transports protons across membranes. *J. Membr. Biol.* 82:179–190. PubMed doi:10.1007/BF01868942

Ramsey, I.S., M.M. Moran, J.A. Chong, and D.E. Clapham. 2006. A voltage-gated proton-selective channel lacking the pore domain. *Nature.* 440:1213–1216. PubMed doi:10.1038/nature04700

Starkov, A.A., V.I. Dedukhova, and V.P. Skulachev. 1994. 6-ketocholestanol abolishes the effect of the most potent uncouplers of oxidative phosphorylation in mitochondria. *FEBS Lett.* 355:305–308. PubMed doi:10.1016/0014-5793(94)01211-3

Vianello, A., F. Macri, E. Braidot, and E.N. Mokhova. 1995. Effect of 6-ketocholestanol on. *FEBS Lett.* 365:7–9. PubMed doi:10.1016/0014-5793(95)00431-8